Iranian Society of Acoustics and Vibration
The 15th International Conference on Acoustics and Vibration ISAV2025
24-25 Dec 2025 Tehran- Iran

Revisiting the Sauerbrey Equation: Insights from Multiphysics FEM Simulation of QCM Crystals

Amirhossein Rabiee[a], Asadollah Kalantarian[b*], Mohammad Bazargan[c], Farhad Khorashe[c]

[a] *Mr., Department of Chemical and Petroleum Engineering, Sharif University of Technology, Tehran, Iran.*

[b] *Dr., Institute for Convergence Science and Technology, Sharif University of Technology, Tehran, Iran.*

[c] *Dr., Department of Chemical and Petroleum Engineering, Sharif University of Technology, Tehran, Iran.*

** Corresponding author e-mail: Kalantarian@sharif.edu*

Abstract

The quartz crystal microbalance (QCM) is a versatile surface-acoustic-wave-based gravimetric sensor widely used in biosensing, vapor and gas detection, thin film monitoring, corrosion studies, polymer adsorption, and surface interaction analysis. In this work, a comprehensive finite element method (FEM) simulation framework for QCM crystals is presented using COMSOL Multiphysics. The model couples solid mechanics, piezoelectricity, and electrostatics to predict resonance behaviour with high accuracy. Validation against analytical calculations showed close agreement, confirming the reliability of the approach. The study further examines the influence of crystal radius on the resonance frequency constant, providing insights into the applicability of the Sauerbrey equation. Results confirm that the Sauerbrey relation underestimates resonance frequency at low diameter-to-thickness ratios because of the edge effect and has relatively low accuracy, while at higher ratios the simulated and analytical values agree within 2.64%. Overall, the proposed FEM framework deepens understanding of QCM behaviour and supports the development of more accurate and efficient sensor designs.

Keywords: Quartz Crystal Microbalance (QCM); Finite Element Method (FEM); Sauerbrey; Surface Acoustic Wave (SAW) Sensors.

1. Introduction

Quartz Crystal Microbalance (QCM) is a sensitive, label-free sensor for tracking nanoscale mass changes at interfaces across a wide range of scientific and engineering problems. Introduced by Günter Sauerbrey in 1959 for gravimetric measurements [1], QCM has since become central to monitoring thin-film growth and deposition processes [2-5] and to probing interfacial phenomena such as adsorption and surface interactions [6-8]. Its ability to provide real-time, label-free detection has also made it invaluable in the study of biomolecular interactions and cellular responses [9-12].

QCM has also been widely applied in chemical and vapor sensing [13-16], in electrochemical and interfacial investigations, including electrodeposition and solution phase measurements [17, 18], in sensor surface engineering using porous and functionalized electrodes [19], and in characterizing viscoelastic behaviour of polymer-loaded resonators [20].

Finite element modelling increasingly complements laboratory work and provides a robust framework for reproducing QCM responses. Simulations enable optimization of sensor geometry and investigation of mass loading, viscoelasticity, and fluid–structure interactions that experiments cannot fully resolve. COMSOL Multiphysics was employed for its modularity, numerical fidelity, and stability to reconcile experimental measurements with spatially and temporally resolved theoretical models.

Finite element modelling of QCM began with a 2D study that showed how a sample of finite lateral size alters resonance frequency and bandwidth through contact area effects and acoustic energy redistribution [21]. Following that work, FEM has been used to numerically and experimentally characterize resonance behaviour and hydrodynamic loading of QCM P devices operating in liquids for biological detection applications [22]. Design and optimization of electrode geometries and high-frequency QCM architectures, including concentric, dual inverted mesa, ringed, and ring dot configurations, have been explored with FEM to enhance energy trapping, increase resonance frequency and quality factor, and tailor mass sensitivity distributions [23-25]. Finite element analyses have specifically examined how electrode material and shape affect local mass sensitivity and overall device performance [26-29]. FEM studies have also modelled functionalized sensing films and coated resonators for gas detection and electronic nose applications to evaluate coating effects on frequency response and selectivity [30]. In liquid environments, finite element approaches addressed thin-layer immobilization, field-deployable pathogen detection concepts, and the influence of droplet wettability and evaporation kinetics on QCM signals [31-33]. Finally, FEM has been applied to investigate the sensing of volumetric liquid properties and the impact of microstructure resonator designs on admittance spectra and mode behaviour [34].

In this paper, we aim to develop a platform for the comprehensive investigation and analysis of QCM crystals using the finite element method (FEM). The accuracy of the model will be tested under various conditions. Upon validation of its performance, we will investigate the effects of different parameters, such as crystal diameter and thickness, on resonance behaviour. The model will be compared with the Sauerbrey equation at varying crystal diameters.

Quartz, being a piezoelectric crystal, experiences shear displacement when an alternating current is applied across its top and bottom electrodes. This alternating current induces resonant oscillations in the quartz crystal, occurring at a frequency known as the resonant frequency. The resonance frequency depends on the crystal's thickness: it increases when the quartz thickness is reduced and decreases when the thickness is increased.

$$f_0 = \frac{\sqrt{\mu_q/\rho_q}}{2t_q} \tag{1}$$

Where t_q, μ_q and ρ_q represent the thickness, shear modulus, and density of the quartz crystal. The resonant frequency of the crystal is inversely proportional to this thickness. To study how the resonant frequency changes with varying quartz thickness across the available quartz substrates, researchers varied the quartz thickness and plotted the corresponding resonant frequency values. In this work, the constants μ_q= 2.947 × 10^{11} g cm^{-1} s^{-2} and ρ_q= 2.648 × g cm^{-3} are used, which are determined by the intrinsic physical properties of quartz.

The theoretical description of a quartz crystal microbalance (QCM) sensor is commonly derived from Sauerbrey's relation, which links the frequency shift to the change in mass on the crystal surface [1]. It is expressed as,

$$\Delta f = -\frac{2{f_0}^2}{\sqrt{\mu_q \rho_q}} \frac{\Delta m}{A} \tag{2}$$

Where A denotes the electrode area of the QCM, Δf represents the variation in resonant frequency, and Δm corresponds to the mass change occurring on the electrode surface.

In this work, a numerical model of the QCM is developed based on FEM and verified against analytical Equations. This work aims to set the ground for enhancements that consider the complicated physics analytical equations do not.

2. Design and Simulation

This section describes the FEM geometry and mesh design, assumptions, governing equations, simulation setup and parameters, mesh-independence test, and validation approach. The model was built in COMSOL Multiphysics 6.1 to simulate coupled multiphysics phenomena.

2.1 Geometry and Meshing

This study models 10 MHz quartz disk resonators with thicknesses 160–171 μm and diameters 1.6–8.2 mm to assess diameter effects on resonance. The disk uses a structured mesh: a central circular region of 207.5 μm meshed with crossed, near-square elements, and an outer annulus divided into 96 equal sectors, each with 100 radial divisions. Mesh density increases toward the center (elements nearly two orders of magnitude smaller than at the perimeter), the surface mesh is extruded into seven thickness layers, and the final mesh is shown in Fig. 1.

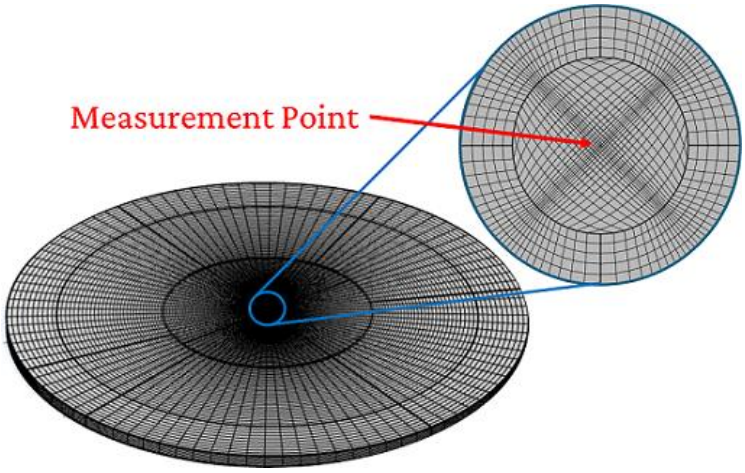

Figure 1. Mesh structure for FEM. The mesh is structured and concentrated in the center. Crystal thickness is made of a number of mesh layers with the same structure.

2.2 Governing Equations

In modelling the quartz crystal microbalance (QCM) under vacuum conditions with the finite element method (FEM), three coupled physical domains must be considered: structural mechanics, electrostatics, and piezoelectric behaviour. These fields are interdependent, and their governing relations are solved simultaneously within the simulation framework. The key equations are summarized below:

A. Charge conservation:

$$\nabla . D = \rho_v \tag{3}$$

Where D denotes the electric displacement vector and ρ_v is the volumetric charge density.

B. Mechanical equilibrium:

$$\nabla . T = 0 \tag{4}$$

With T representing the stress tensor.

C. Piezoelectric constitutive relations (strain–charge form):

$$S = s^E T + d^t E \tag{5}$$

$$D = dT + \epsilon^T E \tag{6}$$

Here, S is the strain tensor, E is the electric field, s^E the elastic compliance at constant electric field, d is the piezoelectric coupling matrix, and ϵ^T the permittivity matrix at constant stress, the superscript t indicates transpose.

2.3 The Assumptions and Parameters of the Simulation

The numerical model was developed under the following assumptions and conditions:
a. The quartz disk is assumed to vibrate in a vacuum environment.
b. A uniform excitation voltage of 10 V peak is applied across the entire disk surface.
c. Sauerbrey's assumptions are adopted. In particular, variations in crystal loading are represented by modifying the crystal thickness, consistent with the requirement that the added mass is rigid and evenly distributed on the surface.
d. Frequency shift is limited to under 5% of the nominal resonance frequency.
e. Displacement measured at the center of the lower face (Grounded) of the disk.
f. The crystal material is AT cut quartz, specified according to the IEEE 1978 standard.
h. Simulations were performed over the frequency range of 9.7–10.1 MHz.

2.4 Mesh Independence and Model Validation

A mesh convergence study verified numerical accuracy by refining an initial 6,200-element mesh progressively in all three directions and generating resonance curves for different mesh intensity factors (Fig. 2). Curves converged as intensity increased, with successive refinements showing negligible differences; plotting resonance frequency versus intensity confirmed consistency. Balancing accuracy and computational cost, an intensity factor of 7 was chosen for subsequent analyses.

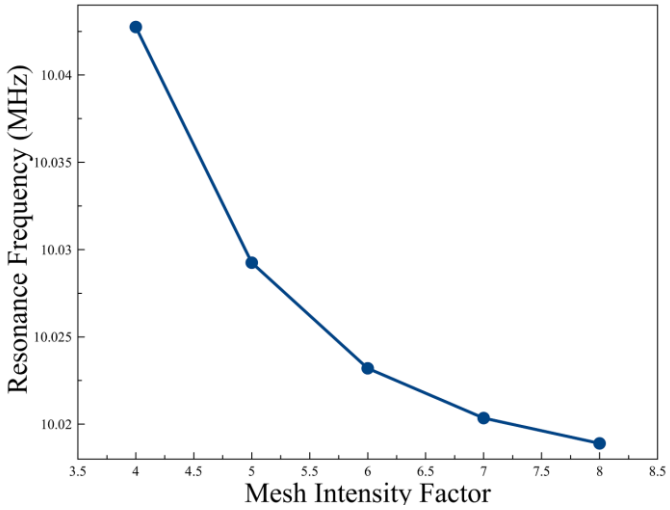

Figure 2. Changes of Resonance Frequency by increasing Mesh Intensity Factor (MIF)

The validated model was then used to examine resonance behaviour. The simulation produced displacement–frequency curves, with Fig. 3 showing the three-dimensional displacement distribution across the disk surface. Fig. 4 illustrates resonance curves obtained for crystals of varying thicknesses, highlighting the sensitivity of frequency response to geometric parameters.

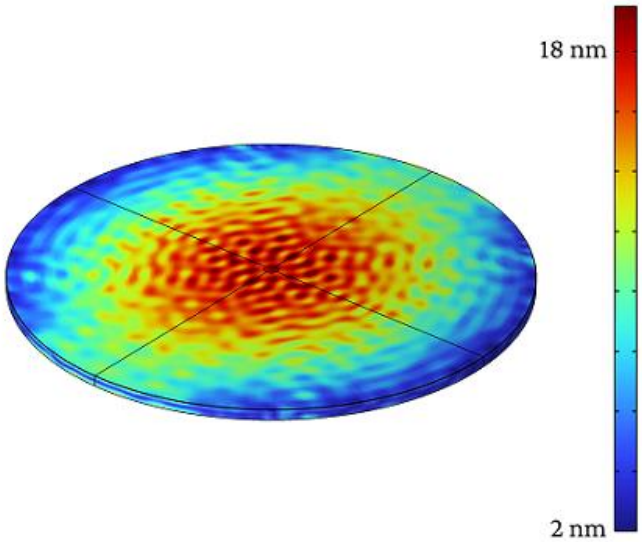

Figure 3. Displacement magnitude at the crystal surface

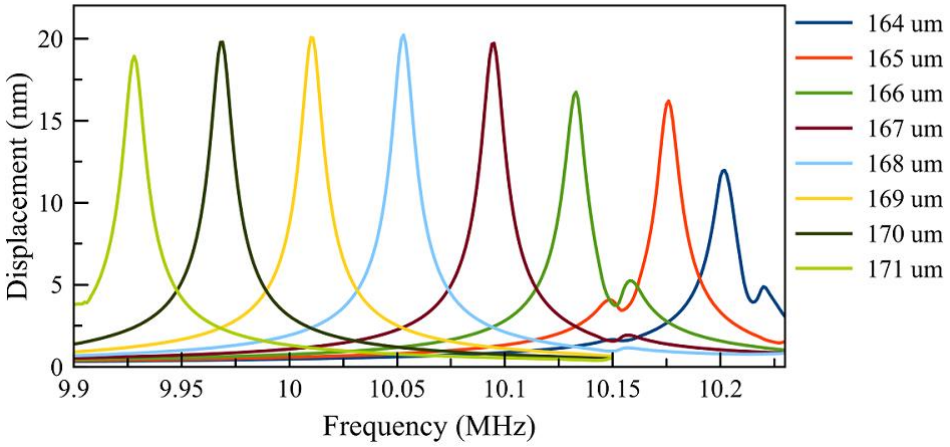

Figure 4. Resonance Curve for Different Crystal Thicknesses. 167 to 169 μm thickness shows a local maximum for the resonance curve quality factor (Peak Height), resulting in better crystal sensitivity. This justifies the relevance of 10 MHz crystals in the market.

3. Results and Discussion

3.1 Crystal Diameter

Based on Eq. 1, the crystal diameter does not directly affect the resonance frequency. However, research indicates that the diameter of the crystal does impact resonance, particularly at small diameter-to-thickness ratios. This phenomenon is referred to as the edge effect by Sauerbrey. [1] To investigate the effect of the crystal edge on the resonance frequency, several simulations were conducted using different crystal diameters ranging from 1.6 mm to 8.2 mm. The base mesh structure was preserved, and the thickness remained fixed at 167 μm. The results indicate a sharp decrease in resonance frequency, which occurs non-monotonically at small diameters. However, as the diameter approaches 8 mm, the behavior stabilizes. Fig. 5 illustrates the relationship between resonance fre-

quency and crystal diameter. Notably, the endpoints of Fig. 5 exhibit approximately a 0.13% difference from the values computed by theory, which falls within an acceptable margin of error.

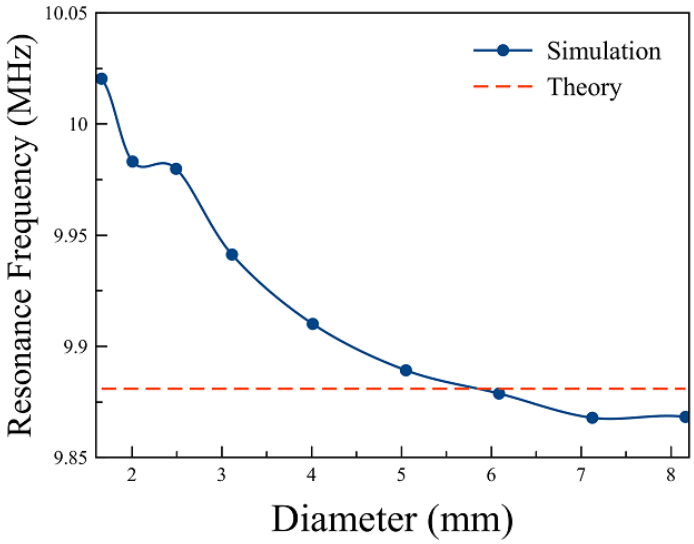

Figure 5. Resonance Frequency Versus Disk Diameter

3.2 Sauerbrey Test

The frequency constant obtained through simulation was compared to values computed using Sauerbrey's equation across a range of crystal diameters. At smaller diameters, there is a significant difference between the two values. However, as the crystal diameter increases, the results from both methods converge, minimizing the error. For diameters larger than 8 mm, the error was approximately 2.64%. Sauerbrey himself acknowledges that his equation is unable to predict the frequency constant accurately for small diameters due to edge effects. The error in the frequency constant calculated by the Sauerbrey equation is high For small diameters and it decreases with increasing disk diameter. For diameter-to-thickness ratios larger than 20 error falls below 1%. [35] A graphical representation of these results is shown in Fig. 6. The error percentage as compared to Sauerbrey's equation for various crystal diameters is represented in Fig. 6.

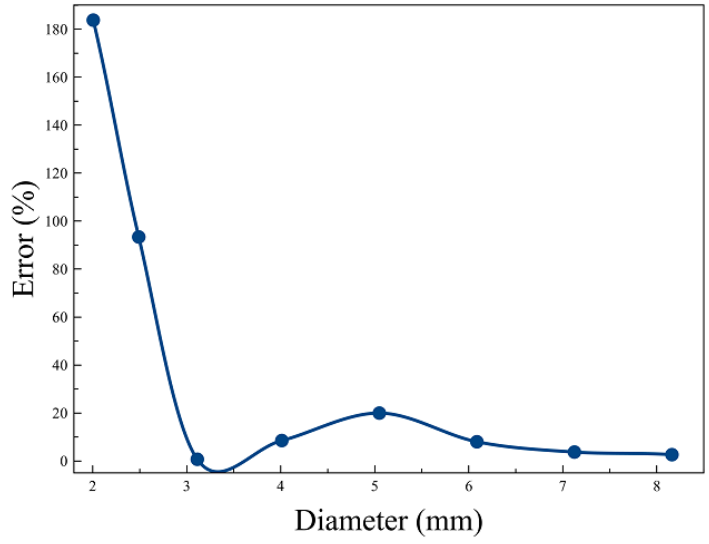

Figure 6. Sauerbrey Test Error for Different Disk Diameters

4. Conclusions

In this study, we developed a three-dimensional numerical model that incorporates solid mechanics and electrostatics for a linear elastic and piezoelectric material known as the Quartz Crystal Microbalance (QCM). The model was implemented using COMSOL Multiphysics. To validate its accuracy, we compared the simulation results with theoretical predictions for resonance frequency. Remarkably, the numerical simulations closely aligned with the theory, exhibiting only 0.7 % error. Our investigation focused on a range of crystal diameters to address the limitations of the Sauerbrey equation in accurately predicting resonance frequencies due to the edge effect. Notably, at large diameters, the resonance frequencies obtained from both the Sauerbrey equation and our simulations matched closely. The error for diameters greater than 8 mm was around 2.64%. However, significant differences emerged at smaller diameters. This is in agreement with Sauerbrey's low accuracy in predicting the frequency constant at small diameters because of the edge effect. This numerical model serves as a foundational framework for further exploration, including the study of liquid interactions with the crystal.

REFERENCES

1. G. Sauerbrey "Verwendung von Schwingquarzen zur Wägung dünner Schichten und zur Mikrowägung", *Zeitschrift für physik*, **155**(2), pp. 206-222 (1959).
2. A. Wajid "Improving the accuracy of a quartz crystal microbalance with automatic determination of acoustic impedance ratio", *Review of scientific instruments*, **62**(8), pp. 2026-2033 (1991).
3. E. Benes, M. Schmid, G. Thorn "Progress in monitoring thin film thickness by use of quartz crystals", *Thin Solid Films*, **174**, pp. 307-314 (1989).
4. I. Kundrata, K. Fröhlich, L. Vančo, M. Mičušík and J. Bachmann "Growth of lithium hydride thin films from solutions: Towards solution atomic layer deposition of lithiated films", *Beilstein Journal of Nanotechnology*, **10**(1), pp. 1443-1451 (2019).
5. K.A. Marx, T. Zhou, A. Montrone and S.J. Braunhut "A Quartz Crystal Microbalance Cell Biosensor: Detecting Nocodazole Dependent Microtubule Disruption Dynamics In Living Cells", *MRS Online Proceedings Library*, **711**, pp. 1-8 (2001).
6. F. Höök, J. Vörös, M. Rodahl, R. Kurrat, P. Böni, J. Ramsden, M. Textor, N. Spencer, P. Tengvall and J. Gold "A comparative study of protein adsorption on titanium oxide surfaces using in situ ellipsometry, optical waveguide lightmode spectroscopy, and quartz crystal microbalance/dissipation", *Colloids and Surfaces B: Biointerfaces*, **24**(2), pp. 155-170 (2002).
7. X. Wang, A. Lamantia, M. Jay, H. Sadeghi, C.J. Lambert, O.V. Kolosov and B.J. Robinson "Determination of electric and thermoelectric properties of molecular junctions by AFM in peak force tapping mode", *Nanotechnology*, **34**(38), pp. 385-704 (2023).
8. M. Doemling, B. Lin, N. Rueger, G. Oehrlein, R. Haring and Y. Lee "Using a quartz crystal microbalance for low energy ion beam etching studies", *Journal of Vacuum Science & Technology A: Vacuum, Surfaces, and Films*, **18**(1), pp. 232-236 (2000).
9. T. Zhou, K.A. Marx, M. Warren, H. Schulze and S.J. Braunhut "The quartz crystal microbalance as a continuous monitoring tool for the study of endothelial cell surface attachment and growth", *Biotechnology Progress*, **16**(2), pp. 268-277 (2000).
10. D. Melendrez, P. Hampitak, T. Jowitt, M. Iliut and A. Vijayaraghavan "Development of an open-source thermally stabilized quartz crystal microbalance instrument for biomolecule-substrate binding assays on gold and graphene", *Analytica Chimica Acta*, **1156**, pp. 338329 (2021).
11. A. Malafronte, F. Auriemma, C. Santillo, R. Di Girolamo, R. Barker, Y. Gerelli and C. De Rosa "Block Copolymers-Based Nanoporous Thin Films with Tailored Morphology for Biomolecules Adsorption", *Advanced Materials Interfaces*, **7**(5), pp. 1901580 (2020).
12. I. Goubaidoulline, G. Vidrich, D. Johannsmann "Organic vapor sensing with ionic liquids entrapped in alumina nanopores on quartz crystal resonators", *Analytical Chemistry*, **77**(2), pp. 615-619 (2005).
13. R.A. Potyrailo, R.J. May, T.M. Sivavec "Recognition and quantification of perchloroethylene, trichloroethylene, vinyl chloride, and three isomers of dichloroethylene using acoustic wave sensor array", *Sensor Letters*, **2**(1), pp. 31-36 (2004).

14. Y. Fu, H.O. Finklea "Quartz crystal microbalance sensor for organic vapor detection based on molecularly imprinted polymers", *Analytical Chemistry*, **75**(20), pp. 5387-5393 (2003).
15. S. Al-Sodies, A.M. Asiri, S.H. Ismail, K.A. Alamry and M.A. Hussein "Development of poly (safranine-co-phenosafranine)/GNPs/MWCNTs nanocomposites for quartz crystal microbalance sensor detection of arsenic (III) ions", *Materials Research Express*, **11**(4), pp. 045701 (2024).
16. J.S. Malhotra, P.H. Reichert, J. Sundberg "A Quartz Crystal Resonator Modified with a Metal-Organic Framework for Sensing of Benzene, Ethylbenzene, Toluene and Xylenes in Water", *2023 IEEE SENSORS*, pp. 1-4 (2023).
17. O. Melroy, K. Kanazawa, J. Gordon and D. Buttry "Direct determination of the mass of an underpotentially deposited monolayer of lead on gold", *Langmuir*, **2**(6), pp. 697-700 (1986).
18. N.P. Cosman, S.G. Roscoe "Electrochemical quartz crystal nanobalance to detect solvent displacement by pH-induced conformational changes of proteins at Pt", *Analytical chemistry*, **76**(19), pp. 5945-5952 (2004).
19. K. Bonroy, J.-M. Friedt, F. Frederix, W. Laureyn, S. Langerock, A. Campitelli, M. Sára, G. Borghs, B. Goddeeris and P. Declerck "Realization and characterization of porous gold for increased protein coverage on acoustic sensors", *Analytical chemistry*, **76**(15), pp. 4299-4306 (2004).
20. M. Skompska, A. Jackson, A.R. Hillman "Evolution from gravimetric to viscoelastic response of poly (3-methylthiophene)-loaded acoustic wave resonators", *Physical Chemistry Chemical Physics*, **2**(20), pp. 4748-4757 (2000).
21. M. Herrscher, C. Ziegler, D. Johannsmann "Shifts of frequency and bandwidth of quartz crystal resonators coated with samples of finite lateral size", *Journal of applied physics*, **101**(11) (2007).
22. P. Wang, J. Su, L. Gong, M. Shen, M. Ruths and H. Sun "Numerical simulation and experimental study of resonance characteristics of QCM-P devices operating in liquid and their application in biological detection", *Sensors and Actuators B: Chemical*, **220**, pp. 1320-1327 (2015).
23. A. Joseph, A. Emadi "Design and optimization of a multichannel quartz crystal microbalance sensor array for multiple target gas detection", *2019 IEEE SENSORS*, pp. 1-4 (2019).
24. W. Pengyi, L. Minghai, L. Mingxiang, W. Leikai and W. Qiang "Design and Simulation of a Piezoelectric Micro-QCM with High Resonance Frequency and Quality Factor", *2020 15th Symposium on Piezoelectrcity, Acoustic Waves and Device Applications (SPAWDA)*, pp. 522-525 (2021).
25. A. Joseph, A. Emadi "A high frequency dual inverted mesa QCM sensor array with concentric electrodes", *IEEE Access*, **8**, pp. 92669-92676 (2020).
26. Q. Chen, X. Huang, Y. Yao and K. Mao "Analysis of the effect of electrode materials on the sensitivity of quartz crystal microbalance", *Nanomaterials*, **12**(6), pp. 975 (2022).
27. J. Hu, X. Huang "QCM mass sensitivity analysis based on finite element method", *IEEE Transactions on Applied Superconductivity*, **29**(2), pp. 1-4 (2018).
28. S. Swaminathan "Development of a Novel Quartz Crystal Microbalance based on Distribution of Mass Loading Area for Improving Mass Sensitivity", Master's Thesis, University of Windsor, Canada (2021).
29. Q. Chen, X.-H. Huang, Y. Yao, K.-B. Luo, H.-Z. Pan and Q. Wang "Ringed electrode configuration enhances the sensitivity of QCM humidity sensor based on lignin through fringing field effect", *IEEE Sensors Journal*, **21**(20), pp. 22450-22458 (2021).
30. A. Das, R. Manjunatha "Modeling of Graphene Oxide Coated QCM Sensor for E-Nose Application", *Recent Trends in Materials: Select Proceedings of ICTMIM 2022*, pp. 179-188 (2022).
31. N. Ghiasi "Modeling of QCM for thin layer immobilization in a liquid environment", Master's Thesis, University of South-Eastern, Norway (2022).
32. H.J. Min, E. Bae "Towards a field deployable pathogen detection system by quartz-crystal microbalance", *Sensing for Agriculture and Food Quality and Safety XIII*, **11754**, pp. 66-72 (2021).
33. B. Murray "Characterization of Evaporation Kinetics and Wettability Using a Quartz Crystal Microbalance", Ph.D. Thesis, Rensselaer Polytechnic Institute, N.Y., USA (2022).
34. N. Mukhin, R. Lucklum "QCM based sensor for detecting volumetric properties of liquids", *Current Applied Physics*, **19**(6), pp. 679-682 (2019).
35. R. Bechmann "Single response thickness-shear mode resonators using circular bevelled plates", *Journal of Scientific Instruments*, **29**(3), pp. 73 (1952).